

Journal of Biomedical Optics

SPIEDigitalLibrary.org/jbo

Morphometric measurement of Schlemm's canal in normal human eye using anterior segment swept source optical coherence tomography

Guohua Shi
Fei Wang
Xiqi Li
Jing Lu
Zihua Ding
Xinghuai Sun
Chunhui Jiang
Yudong Zhang

Morphometric measurement of Schlemm's canal in normal human eye using anterior segment swept source optical coherence tomography

Guohua Shi,^{a,b,*} Fei Wang,^{c,*} Xiqi Li,^{a,b} Jing Lu,^{a,b}
Zhihua Ding,^d Xinghuai Sun,^c Chunhui Jiang,^c and Yudong Zhang^{a,b}

^aChinese Academy of Sciences, The Key Laboratory on Adaptive Optics, Chengdu 610209, China

^bInstitute of Optics and Electronic, Chinese Academy of Sciences, Chengdu 610209, China

^cFudan University, Department of Ophthalmology and Vision Science, Eye & ENT, Shanghai 200031, China

^dZhejiang University, State Key Laboratory of Modern Optical Instrumentation, Hangzhou 310027, China

Abstract. We have used anterior segment swept source optical coherence tomography to measure Schlemm's canal (SC) morphometric values in the living human eye. Fifty healthy volunteers with 100 normal eyes were measured in the nasal and temporal side. Comparison with the published SC morphometric values of histologic sections proves the reliability of our results. The statistical results show that there are no significant differences between nasal and temporal SC with respect to their diameter, perimeter, and area in our study (diameter: $t = 0.122$, $p = 0.903$; perimeter: $t = -0.003$, $p = 0.998$; area: $t = -1.169$, $p = 0.244$); further, no significant differences in SC morphometric values are found between oculus sinister and oculus dexter (diameter: $t = 0.943$, $p = 0.35$; perimeter: $t = 1.346$, $p = 0.18$; area: $t = 1.501$, $p = 0.135$). © 2012 Society of Photo-Optical Instrumentation Engineers (SPIE). [DOI: 10.1117/1.JBO.17.1.016016]

Keywords: optical coherence tomography; ophthalmology; Schlemm's canal; morphometry; glaucoma.

Paper 11592L received Oct. 11, 2011; revised manuscript received Dec. 4, 2011; accepted for publication Dec. 8, 2011; published online Feb. 9, 2012.

Glaucoma is a major blinding disease that causes irreversible bilateral blindness in at least 6.8 million people.¹ High intraocular pressure (IOP) is the leading reason for the formation of glaucoma.² Aqueous outflow (AO) is the key regulator of IOP; it operates by means of the trabecular meshwork (TM) draining into Schlemm's canal (SC) and then to the collector channels (CC), which empty into scleral veins.³ SC is like a relay station of aqueous. Thus its size is related to outflow facility, and may have something to do with IOP.⁴ Therefore, imaging SC and measuring its size could be an important tool for glaucoma diagnosis and treatment, but it requires resolution in the range of tens of micrometers. For this reason, studies have been limited to histologic sections or animal eye.^{5,6} Allingham et al. have examined the correlation between outflow facility and morphometric values of SC in normal and primary open angle glaucoma (POAG) human donor eyes.⁵ A statistically significant correlation was found between facility and SC area, and POAG eyes had a significantly smaller SC area, SC perimeter, and SC inner wall length compared with normal eyes. It would be reasonable to assume that examination of the correlation between outflow facility and morphometric measurement of SC in normal and glaucomatous living eyes could be used as further rationale to support earlier treatment for individuals with suspected POAG.

With the emergence of Fourier domain optical coherence tomography (FDOCT), the image speed and sensitivity of optical coherence tomography (OCT) have been revolutionized in

last few years and have led to successful implementation of SC imaging *in vivo*.^{7,8} Kagemann et al. were the first to noninvasively measure the SC area using commercial 840-nm spectral domain optical coherence tomography (SDOCT; Biotigen Inc., USA) in living human eye.⁷ By using SDOCT Doppler measurement, they accurately identified the SC, CCs, and scleral veins, and measured the morphometric values of SC area. Asrani et al. have established a set of 1.3- μm swept source OCT (SSOCT).⁸ The 1.3- μm wavelength light enhances the penetration depth and system Signal to Noise Ratio in the anterior segment. This leads to both eyes' SC, and the TM were visualized in all of the patients with glaucoma.

In this study, a 1.3- μm SSOCT was developed to image the anterior segment in living human eye. High-speed, high-resolution imaging of the ocular anterior segment *in vivo* was achieved by SSOCT. Both eyes of 50 healthy subjects were imaged nasally and temporally, and the cross-sectional images permit the visualization of SC in both eyes. The morphometric values of SC were calculated successfully.

As is shown in Fig. 1(a), the SSOCT system is based on a swept source laser (HSL-2000; Santec). The swept source is centered at 1310 nm, with a wavelength scan range of approximately 110 nm that achieves 6.78- μm axial resolution in air theoretically. A Michelson interferometer (INT-MSI-1300; Thorlabs) with a balance detector is used to detect the signal. A laser diode with 660-nm wavelength functions as an aiming laser. A photo diode is used to detect optical power to ensure that the light incident to the cornea is safe. In order to compensate the polarization mode dispersion of the whole system, a fiber polarizer control is applied in the sample path to control the polarization. A Mach-Zehnder interferometer (INT-MZI-1300;

*Guohua Shi and Fei Wang contributed equally to this work.

Address all correspondence to: Guohua Shi, Chinese Academy of Sciences, Chengdu 610209, China; or Chunhui Jiang, Department of Ophthalmology and Vision Science, Eye & ENT, Fudan University, Shanghai 200031, China. Tel: 0086-28-8510-0630; Fax: 0086-28-8510-0433; E-mail: guohua_shi@yahoo.com.cn

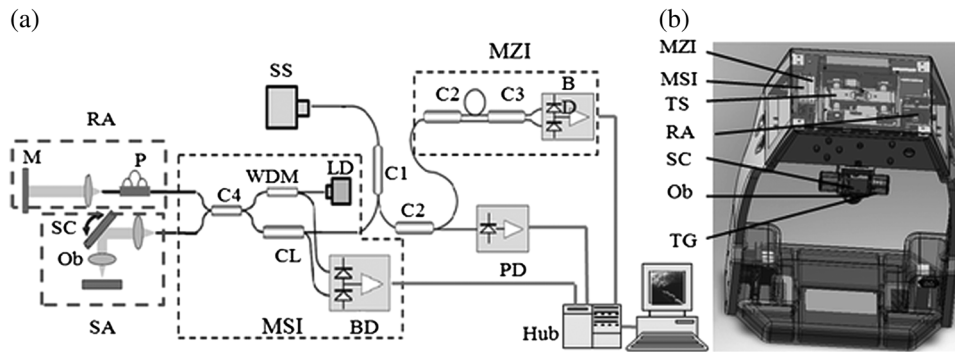


Fig. 1 (a) Schematic of SSOCT system; (b) structure diagram of SSOCT system. SS, swept source; C1, fiber coupler (5/95); C2 ~ C4, fiber coupler (50/50); BD, balance detector; PD, photo diode; LD, laser diode; WDM, wavelength division multiplexer; CL, circulator; P, polarization controller; M, Mirror; SC, x-y scanner; Ob, objective; MZI, Mach-Zehnder interferometer; MSI, Michelson interferometer; RA, reference arm; SA, sample arm; TS, 3-dimensional electric translation stage; TG, target.

Thorlabs) is used to calibrate the wavelength to enhance the actual axial resolution. After calibration the actual axial resolution is $8.03 \mu\text{m}$ in air, which is equal to $6.0 \mu\text{m}$ in SC because the refractive index of aqueous is 1.34. Each A-line contains 512 pixels, and the typical B-Scan image contains 800 A-lines. The system frame rate is 22.5 frames per second. The real-time frame rate reduces the influence of eye jitter.

Furthermore, the morphometric measurement of SC is incident beam angle dependent. Therefore, in order to minimize the variation of incident beam angle, a gantry structure is utilized. As is shown in Fig. 1(b), the MSI, MZI, and reference arm are fitted in a motherboard. The gantry structure allows the object to lie down. When beginning the experiment, the fixation target turns on the LED, so the object can stare the LED. This means that all the subjects are in the state of emmetropia while imaging. The sample arm is connected to a three-dimensional electric translation stage, which is manually controlled by six buttons on the frontal control panel to adjust the imaging location and focusing position to make the scanning plane (B-scan) orthogonal to the SC orientation.

To ensure the accuracy of morphometric measurement, the impact of refractive index must be considered. Therefore, the axial and transverse scan ranges of SSOCT should be calibrated carefully. The typical cross-section image consists of 800 A-lines, and each A-line contains 512 pixels. The axial scan range is 2.97 mm in air. Thus, by considering the refractive index of aqueous, each pixel represents $4.3 \mu\text{m}$ length in axial when the pixel is in inside the SC. The transverse scan range is 4.8 mm in air, so each pixel represents $6\text{-}\mu\text{m}$ length in transverse.

Figure 2 shows the image of the anterior segment. As is shown in Fig. 2, the outline of SC is defined as a white slit-like structure located anterior to the peripheral part of the trabecular meshwork, which is between the sclera spur and Schwalbe's line. When we carry out the morphometric measurement, we zoom in the image and use a polygon to draw the profile of SC manually. Then the diameter can be obtained by the farthest distance of the two pixels, the perimeter can be obtained by the sum of distances, and the area can be obtained by the polygonal area formula as Eq. (1) shows:

$$S_{\Omega} = \frac{1}{2} \sum_{i=1}^M (x_i \times y_{i+1} - x_{i+1} \times y_i) d_x d_y, \quad (1)$$

where x_i and y_i are the pixels' coordinates, and d_x and d_y are the length that each pixel represented in transverse and axial, respectively.

This research was approved by Institutional Review Board of Eye and ENT Hospital of Fudan University and followed the tenets of the Declaration of Helsinki. Informed consent was signed by each subject. Fifty healthy subjects were recruited, and the male to female ratio was 1:1. All of the subjects were checked by frequency doubling technology perimeter and Humphrey field analyzer to make sure that the subjects did not suffer from glaucoma. The IOP of subjects in this study was in the range of 10 to 21 mm Hg (average, $15.37 \pm 2.72 \text{ mm Hg}$). The age of subjects was in the range of 21 to 74 yr (average, 44.86 ± 17.55).

All 50 healthy subjects permitted the visualization of SC in both eyes nasally and temporally, and each side was measured twice to get the average value for further analysis. Therefore we obtained four sets of measurements. There are SC morphometric values of ODN, ODT, OSN, and OST, respectively; these are shown in Fig. 3. SPSS13.0 (SPSS Inc., Chicago, IL) was used in the analysis. A p value less than 0.05 was considered statistically significant. All statistics tests adopt two-tailed test. After Shapiro-Wilk test, normal distribution materials are described as mean \pm standard deviation. The statistical results of SC morphometric values are shown in Table 1.

Allingham et al. have carried out a detailed SC morphometric measurement among 10 normal human donor eyes, and have given out averages of the SC diameter, perimeter, and area.⁵ The SC area and diameter of donor eyes will be different

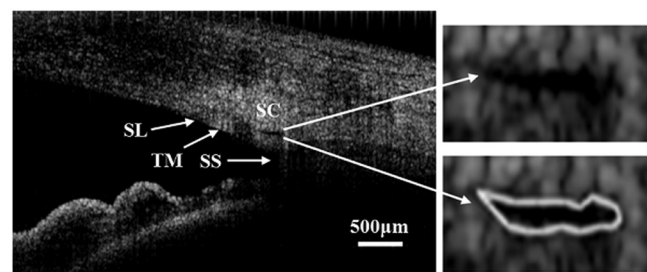


Fig. 2 The SSOCT image of the anterior segment in living human eye. The image of temporal side of oculus dexter: Subject 20; Age: 26; sex: male; IOP: 14 mm Hg; diameter: $271.06 \mu\text{m}$; perimeter $555.5 \mu\text{m}$; area: $7776 \mu\text{m}^2$. SC, Schlemm's canal; SL, Schwalbe's line; TM, trabecular mesh; SS, scleral spur.

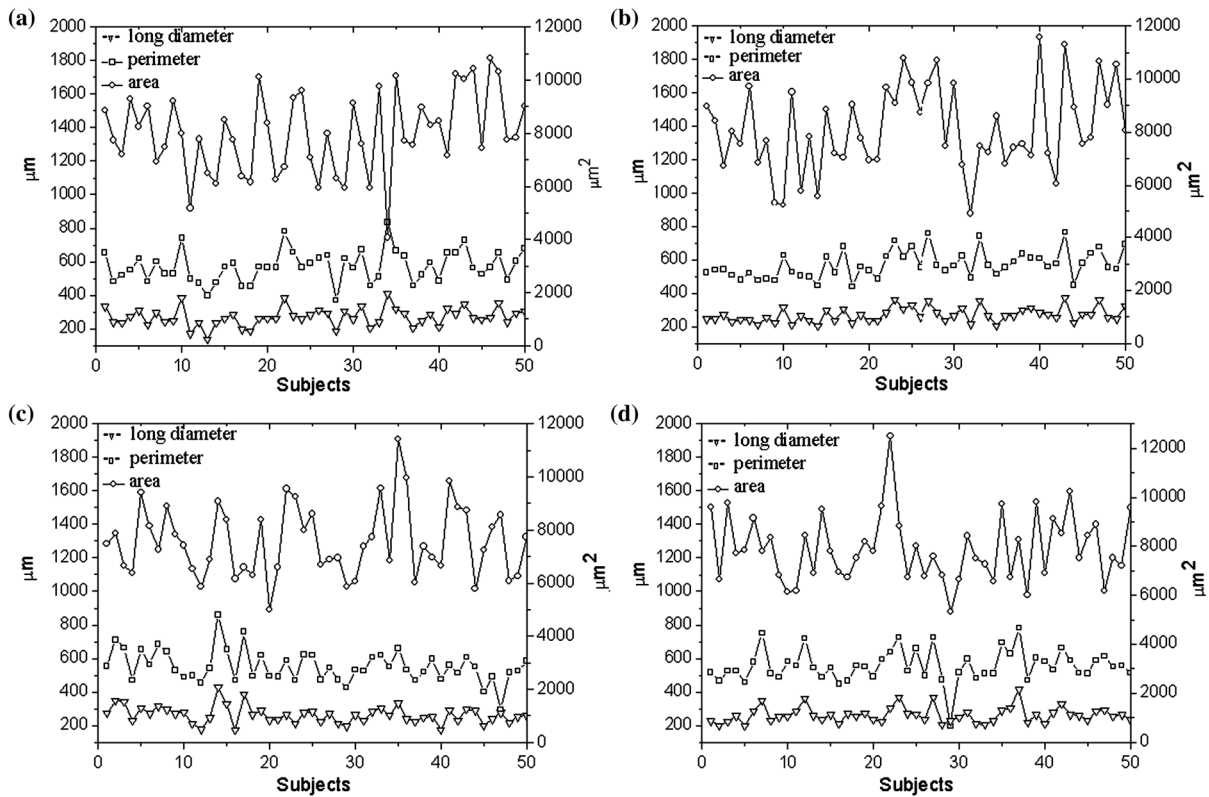


Fig. 3 The morphometric values of SC. (a) nasal of oculus dexter (ODN); (b) temporal of oculus dexter (ODT); (c) nasal of oculus sinister (OSN); (d) temporal of oculus sinister (OST). Circles represent the area value; squares are the perimeter value; triangles are the diameter.

with the living normal human eyes. The perimeter, on the other hand, should be close to the average measurement, because the cross-section of SC is a naturally occurring cavity. After averaging OD and OS perimeter values, the average perimeter value given out by Allingham et al. is $520 \pm 114 \mu\text{m}$, and our result is $563.42 \pm 92.35 \mu\text{m}$. The values are close to each other. Furthermore, Kagemann et al. obtained the average SC area

of 21 normal living subjects: $7254 \pm 2605 \mu\text{m}^2$ (Ref. 8). Our statistical result of averaging SC area is $7888.38 \pm 1472.58 \mu\text{m}^2$. These values are also close to each other. These comparisons proved the reliability of our results.

However, Kagemann et al. concluded that nasal SC areas were significantly larger than temporal ones.⁸ In our study, although a number of SC area values from several subjects

Table 1 Statistical results of normal subjects.

	SC diameter (Mean ± SD)	SC perimeter (Mean ± SD)	SC cross section area (Mean ± SD)
ODN	270.66 ± 55.47	573.827 ± 95.22	7972.4 ± 1526.99
ODT	269.88 ± 44.10	570.55 ± 81.22	8116 ± 1626.99
OSN	264.12 ± 51.30	552.98 ± 95.00	7561.12 ± 1343.44
OST	263.19 ± 47.68	556.32 ± 97.13	7904 ± 1362.56
OD	270.27 ± 49.86	572.19 ± 88.06	8044.2 ± 1570.94
OS	263.66 ± 46.28	554.65 ± 96.09	7732.56 ± 1357.18
Nasal	267.39 ± 53.26	563.4 ± 95.7	7766.76 ± 1445.71
Temporal	266.54 ± 45.83	563.45 ± 89.36	8010 ± 1496.29
Average	266.96 ± 49.55	563.42 ± 92.35	7888.38 ± 1472.58

The values shown are mean ± SD. The values of "OD" are obtained by averaging values of each ODN and ODT values, and the values of "nasal" are obtained by averaging values of each ODN and OSN values. The same definitions are made for the values of "OS" and "temporal." "Average" values are obtained by averaging values for each OD and OS values.

(such as Subjects of 9, 10, 19, 20, 26, 27, etc.) show the significant difference between nasal and temporal side, the statistical results of 100 eyes indicate that there are no significant differences between nasal and temporal side with respect to SC diameter, perimeter, and area (diameter: $t = 0.122$, $p = 0.903$; perimeter: $t = -0.003$, $p = 0.998$; area: $t = -1.169$, $p = 0.244$). Additionally, no differences were found in the SC statistical values between OS and OD (diameter: $t = 0.943$, $p = 0.35$; perimeter: $t = 1.346$, $p = 0.18$; area $t = 1.501$, $p = 0.135$).

In conclusion, we have imaged SC and measured its morphometric values successfully by SS-OCT system in the living human eye. These values are useful for determining the impact of SC morphometric on flow resistance, and assist in understanding the role of SC size for POAG. To the best of our knowledge, this is the first noninvasive SC morphometric measurement by SSOCT in Asian subjects. These kinds of measurements are still new and non-standard, so this study will be a good reference for future research. However, the eye jitter, breath, and calibration accuracy of scan range have a large impact on the measurement result. Furthermore, it is actually impossible to maintain the absolute verticality between the scanning plane (B-scan) and the SC orientation in living human eye. Thus, this approach needs further improvement to enhance its absolute accuracy. At the same time we will analyze the correlation between the age, IOP, and SC morphometric values, and make a detailed comparison of SC morphometric values between normal and POAG human eyes.

Acknowledgments

This work was supported by the National Science Foundation of China (Grant No. 61108082) and the Knowledge Innovation Program of the Chinese Academy of Sciences (Grant No. KG CX2-Y11-920).

References

1. H. A. Quigley and A. T. Broman, "The number of people with glaucoma worldwide in 2010 and 2020," *Br. J. Ophthalmol.* **90**(3), 262–267 (2006).
2. A. Sommer et al., "Relationship between intraocular pressure and primary open angle glaucoma among white and black Americans," *The Baltimore Eye Survey. Arch. Ophthalmol.* **109**(8), 1090–1095 (1991).
3. W. M. Grant, "Clinical measurements of aqueous outflow," *AMA Arch. Ophthalmol.* **46**(2), 113–131 (1951).
4. M. C. Johnson and R. D. Kamm, "The role of Schlemm's canal in aqueous outflow from the human eye," *Invest. Ophthalmol. Vis. Sci.* **24**(3), 320–325 (1983).
5. R. R. Allingham, A. W. de Kater, and C. R. Ethier, "Schlemm's canal and primary open angle glaucoma: correlation between Schlemm's canal dimensions and outflow facility," *Exp. Eye Res.* **62**(1), 101–109 (1996).
6. O. Mäepea and A. Bill, "Pressures in the juxtacanalicular tissue and Schlemm's canal in monkeys," *Exp. Eye Res.* **54**(6), 879–883 (1992).
7. L. Kagemann et al., "Identification and assessment of Schlemm's canal by spectral domain optical coherence tomography," *Invest. Ophthalmol. Vis. Sci.* **51**(8), 4054–4059 (2010).
8. S. Asrani et al., "Detailed visualization of the anterior segment using Fourier-Domain optical coherence tomography," *Arch. Ophthalmol.* **126**(6), 765–771 (2008).